ACS APPLIED MATERIALS & INTERFACES

Research Article

www.acsami.org

Interaction of Novel Fluorescent Nanoscale Ionic Silicate Platelets with Biomaterials for Biosensors

Hsiao-Chu Lin,[†] Jiang-Jen Lin,*[,†] and Yu-Jane Sheng*[,†,‡]

[†]Institute of Polymer Science and Engineering, National Taiwan University, Taipei, 10617, Taiwan

[‡]Department of Chemical Engineering, National Taiwan University, Taipei, 10617, Taiwan

Supporting Information

ABSTRACT: The nano silicate platelets (NSPs) of 100 × 100 × 1 nm^3 in dimension were previously derived from the exfoliation of naturally occurring sodium montmorillonite clay, and their affinity to the surface of bacteria was revealed. The unique characteristics of ionic charges (≡Si−O−Na^+) and the presence of siloxanol functionalities (≡Si−OH) allowed the organic modification of NSP to form NSP-tethering poly(hydroxyethyl methacrylate) (PHEMA) pendants through a sol−gel and living polymerization. By attaching nathphalimide-type fluorescence onto NSP-PHEMA, a new class of fluorescent organic−inorganic hybrid (NSP-PHEMA-HA), was prepared and its photoluminescence (PL) and bacterial trapping properties were characterized. The investigation of PL emission revealed that the fluorescent NSP hybrids could be used to detect bacteria and possess the potential for the biosensor applications.

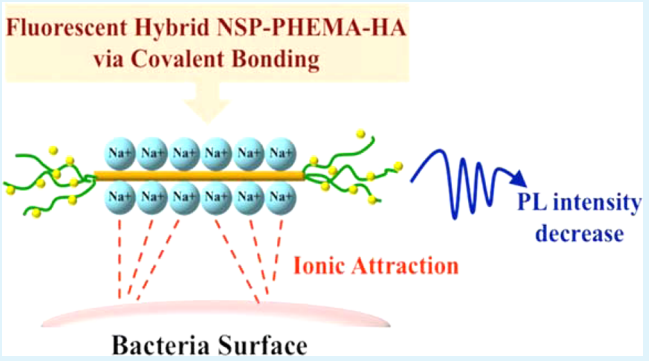

KEYWORDS: *nano silicate platelet, clay, PHEMA, photoluminescence, physical trapping*

INTRODUCTION

Detection of potentially harmful microorganisms that may cause diseases[1,2] is an important research subject. The conventional methods used clinically for the detection of pathogenic bacteria, such as *Escherichia coli* (*E. coli*), rely on culturing bacteria in growth medium. However, the process can take days to be completed,[3] thus the methods for pathogen recognition such as fluorescent-labeling antibodies,[4−6] DNA probes,[7,8] or bacteriophages[9] have been actively pursued.

Recent developments on finding new nanomaterials that are at least one dimension in the range of 1 to 100 nm may offer new insights in understanding the occurrence and the transformation of biomaterials in biological system due to their similarity in sizes.[10,11] The two-dimensional silicate clay minerals with layered structure and thin platelet shape of the fundamental unit are particularly interesting nanomaterials with respect to their high affinity toward polar organics such as DNA and proteins. The high surface area, ionic character, and layered structures of the silicate clays are characteristic features for immobilizing proteins. Moreover, the ionic types of clays including anionic layered double hydroxide (LDH) and cationic sodium montmorillonite (Na^+-MMT) are known for their ability to adsorb biomaterials.[12,13] In our earlier research, encapsulating the bovine serum albumin (BSA) by polyamine intercalated MMT were discussed.[14,15] Our recent findings on the bacterial capturing mechanism by clays also implied the intimate interaction between silicate clays and microorganisms.[16]

The fundamental silicate platelets (~1 nm in thickness) with an extremely large surface area (~720 m^2/g)[17,18] are size compatible for many biomaterials, for example, SARS (severe acute respiratory syndrome) virus (80 nm).[19] It has been suggested that the layered clays with the intercalated cetylpyridinium cationic organics in the gallery are effective for adsorbing microorganisms.[20] Our recent studies on polymer modification have led to the clay exfoliation and the isolation of nanometer-thick silicate platelets (NSPs).[21−23] The nanoplatelets are thin and with ionically charged surface, unlike the pristine form of layered structure in Na^+-MMT primary units. The complete exposure of previously sequestered surface charges allows the intensive surface interaction with the polar organics.[16]

In literature, the surface initiated polymerization was reported for grafting the solid surface with polymeric brushes on layered silicate clays by free radical polymerization[24] and living polymerization methodologies that include anionic living polymerization,[25] nitroxide-mediated polymerization,[26,27] reversible addition−fragmentation chain transfer,[28] and atom transfer radical polymerization.[29,30] They generally involved the ionic bonding between the polymers and the silicate surface through ionic exchange reaction of the initiator with the sodium counterions in the clay gallery in the first step. The preliminary

Received: January 30, 2015
Accepted: May 4, 2015
Published: May 4, 2015

DOI: 10.1021/acsami.5b00796
ACS Appl. Mater. Interfaces 2015, 7, 10771−10778

Scheme 1. Conceptual Diagram of Preparation of NSP-PHEMA-HA by Sol–Gel and ATRP

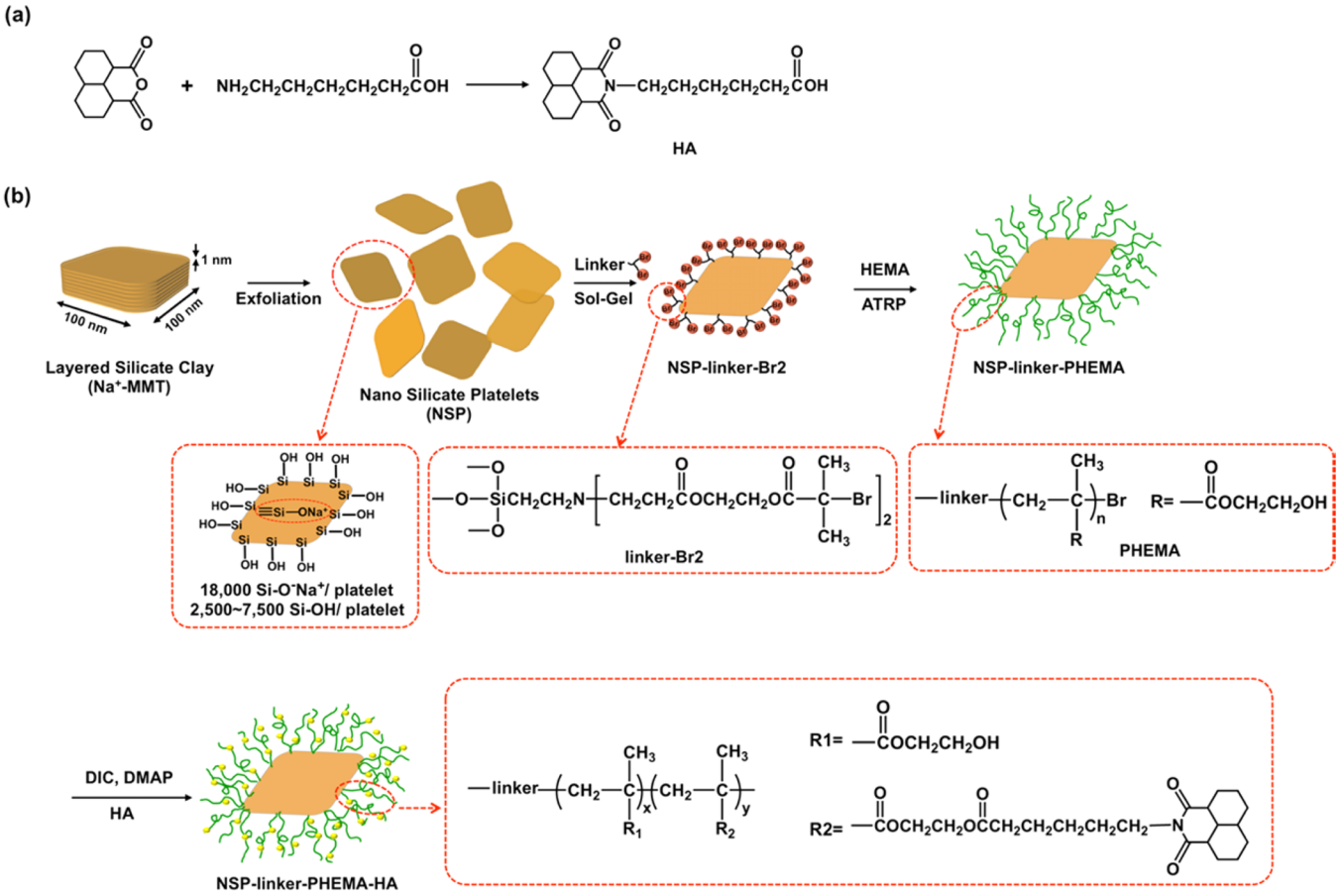

work was reported for growing polymer brushes by covalent bonding onto platelet silicates through the silanol (≡Si–OH) groups on the clay sheets.[31,32] The living polymerization technique was effective for grafting organic moieties to NSP through a linker with covalent bonding to the silicate platelets.[33]

For the clay–bacterial interaction, it was demonstrated that silicate platelets are with low cytotoxicity and genotoxicity.[34] However, the nanoplatelets derived from the clay exfoliation could exhibit the antimicrobial properties by a proposed physical capturing mechanism due to the high affinity of thin silicate platelets in association with the near-by bacteria.[16] These observations prompted us to develop biomedical applications by tailoring the silicate nanoplatelets via grafting with hydrophilic poly(2-hydroxyethyl methacrylate) (PHEMA) hydrogels that was used in a wide range of biomedical applications.[35] In this study, atom transfer radical polymerization (ATRP) was carried out to grow the PHEMA chains and generate a novel class of organic–inorganic material. Then the athphalimide-type fluorescent 6-(1,3-dioxo-1*H*-benzo[de]-isoquinolin-2(3*H*)-yl)hexanoic acid (HA) was bonded for potential sensor uses.

EXPERIMENTAL SECTION

Materials and Methods. The Materials and procedure for preparing NSP-PHEMA hybrid is similar to the process performed in our previous studies.[23] The details of the procedure are also listed in the Supporting Information (S.1–S.4).

Preparation of Fluorescent NSP-PHEMA-HA. 6-(1,3-Dioxo-1*H*-benzo[de]isoquinolin-2(3*H*)-yl)hexanoic acid (HA) was synthesized by 1,8-naphthalic anhydride (5.0 g, 0.025 mol) and 6-aminocaproic acid (3.3 g, 0.025 mol) in dimethylformamide (DMF) (20 mL) which were stirred vigorously at 50 °C for 3h and then reactor was maintained at 150 °C for 3 h. The product mixture was subjected to high vacuum oven to remove DMF and get yellow solids, HA. NSP-PHEMA (1.0 g) were dispersed in DMF (10 mL) and then doped 20% HA (0.0080 g, 0.026 mmol) that reacted with *N*,*N*′-diisopropylcarbodiimide (DIC) (0.0036 g, 0.028 mmol) and 4-dimethylaminopyridine (DMAP) (0.0034 g, 0.0028 mmol) at 120 °C for 12 h to get the clay slurry. (Scheme 1) Washing at DMF and isolating by centrifugation purified the product. After purification, NSP-PHEMA-HA dispersed in deionized water.

Ionic Exchange of Na^+-NSP by 1-Aminopyrene-salts. 1-Aminopyrene was acidified by HCl and bonded to Na^+-NSP by ionic exchange. Na^+-NSP (2.0 g, 120 mequiv./ 100 g) was dispersed in 180 mL of deionized water. 1-Aminopyrene (0.26 g, 1.2 mmol) was prepared in deionized water (20 mL) and treated in a separate flask with HCl (35%, 0.12 g, 1.2 mmol). While the clay slurry was vigorously stirred, 1-aminopyrene-salts solution was added rapidly into clay slurry at 80 °C and the temperature was maintained for 5 h. The solid precipitates NSP-pyrene were filtered and washed several times with deionized water to remove the byproduct sodium chloride.

Preparation of Bacterial Cultures. The Gram-negative bacteria, *E. coli*, were cultured at 37 °C on LB plates (Luria–Bertani broth with 1.5% agar). Each bacterial sample was added to a culture tube containing 10 mL of LB. The inoculated tube was kept at 37 °C and shaken for 24 h. The culture was maintained overnight in LB broth, and then 100 μL of the broth was transferred into fresh medium to restart the cell cycle. After 3 h incubation at 37 °C, the cells were measured by analyzing the optical density at 600 nm (OD600), and the data was synchronized at the log phase of the growth curve. Note that the Gram-positive bacteria, *Staphlycoccus aureus*, were prepared by the same methods as *E. coli*.

DOI: 10.1021/acsami.5b00796
ACS Appl. Mater. Interfaces 2015, 7, 10771–10778

SEM Observation Experiments of NSP-PHEMA-HA with Bacterial. Suspensions of *E. coli* and *S. aureus* were adjusted to 10^6 CFU/mL, yielding final clay composites concentrations of 0.05 wt %, respectively. A 5 mL portion of the bacterial suspension was then transferred to a 6 cm dish with a 22 mm square glass coverslip (Matsunami, Japan) in each dish. A sample of 10^6 CFU/mL bacteria in 0.85% saline solution was added to the control well. Samples of bacterial broth were removed at 0 and 1h. The samples were left on the glass, fixed with 2.5% glutaraldehyde, and stored overnight at 4 °C. The fixed samples were then washed three times with water and dehydrated two times each with 80%, 95%, and 100% ethanol solution, followed by field emission-scanning electron microscopy (FE-SEM).

Characterizations. Fourier-transform infrared (FT-IR) spectra were recorded on a PerkinElmer Spectrum One FT-IR spectrometer over the range 400−4000 cm^{-1}. The organic content was analyzed by TGA on a PerkinElmer Pyris 1 Instrument. The temperature was increased from 100 to 900 °C at 10 °C/min in air. Aqueous dispersions of the nanohybrids (0.005 wt %) were monitored from 300 to 700 nm by UV−visible spectrophotometer (Shimadzu UV mini 1240). 10^5, 10^6, 10^7 CFU/mL bacteria was added into 0.005 wt % clay nanohybrids in a culture tube, respectively. The inoculated tube was kept at 37 °C and shaken for 1 h. The fluorescent features of nanohybrids were measured by Fluorolog Tau-3 Lifetime SystemA. ZetaPlus zetameter (Brookhaven Instrument Corp.,NJ) was used for characterizing the ionic property of NSP-Pyrene. The zeta potentials of NSP-Pyrene in aqueous suspension of 0.01 wt % concentration were measured from pH 2 to 11. Aqueous hydrochloric acid (HCl) and sodium hydroxide (NaOH) solution were used to adjust the pH of clay suspensions. The reliability of the zeta potential measurements was controlled with standard deviation of reading less than 2. Scanning electron microscope (SEM) was performed on a JEOL JSM-5600 SEM system and operated at 15 kV. The samples were coated with Pt before the SEM measurements.

RESULTS AND DISCUSSION

Synthesis and Characterization of NSP-PHEMA-HA. The silicate nanoplatelets were grafted by poly(hydroxyethyl methacrylate) pendants (PHEMA) polymer via a linker of bromide and triethoxysilane functionalities and followed by atom-transfer radical polymerization (ATRP) of hydroxyethyl methacrylate monomer. The characterization of the two bromide linkers and the linker bonded to NSP were analyzed by IR and NMR in our previous study. And the amounts of polymer can be adjusted by the molar ratio of initiator/monomer.[33] In this research, the grafting of HEMA polymers was conducted in MeOH/H_2O (5/5, w/w) with a CuCl/dpy catalyst at ambient temperature (Scheme 1b). And the NSP-PHEMA was adjusted to have the composition of 50/50 by weight of the tethered polymer to clay. The hybrid was dispersible in DMF and bonded with HA according to the procedures described in the Experimental Section. The grafted PHEMA-HA exhibited the hydroxyl groups (−OH) and the carbonyl groups (C═O) at 3100−3500 and 1740 cm^{-1} respectively (Figure 1a). According to the fluorescence of HA, the UV−vis spectra showed an absorbance at 280 and 330 nm (Figure 2a). We use the fluorescence excitation bonds around 280 and 330 nm. It can be obviously observed that there was no fluorescence when using 280 nm as excited wavelength. But intense fluorescence was seen when excited by 330 nm wavelength and the emission bonds were around 380 to 480 nm. When the concentration was increased, the intensity of the fluorescence was increased as shown in Figure 2b. It suggested that NSP-PHEMA-HA were dispersed well in the aqueous solutions. From the result above, we selected 330 nm as exciting wavelength.

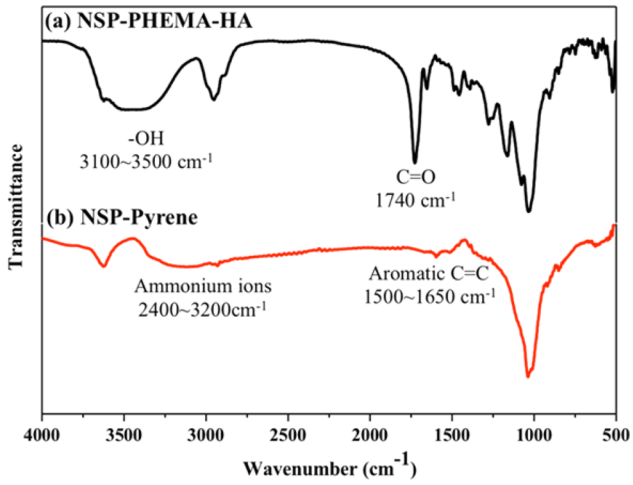

Figure 1. FTIR spectra of NSP-PHEMA-HA and NSP-pyrene.

Synthesis and Characterization of NSP-Pyrene. Beside the covalent bonding modification of NSP, the ionic exchange method was used. According to our previous report, the exfoliation of layered Na^+-MMT using a two-step procedure involving ionic exchange exfoliation of the layered silicate stacks into individual platelets.[19] The silicate platelets have uniquely combined physical traits of large surface area (~750 m^2/ g) and intense surface anionic charges (~18 000 charges/platelet). On the basis of a cationic exchange capacity (CEC) of 1.2 mequiv/g, the sodium cations on NSP were exchanged with 1-aminopyrene/HCl salts. (Scheme 2) The NSP-pyrene was obtained and analyzed by FTIR, displaying the absorption at 2400−3200 cm^{-1} and 1500−1650 cm^{-1} that were characteristic of the ammonium ions ($-NH_3^+$) and the double bonds of aromatic rings (C═C) respectively (Figure 1b). From the UV−vis spectra, it had two specific absorbed peaks at 280 and 350 nm (Figure 3a). Using these two peaks as excited wavelengths, there was an intense emission peak around 400−500 nm when the excited wavelength was 350 nm and only weak fluorescence was observed under excited wavelength of 280 nm. The intensities of fluorescence were not systematically increased when the concentrations were increased (Figure 3b). Since the pyrene functionalities are hydrophobic in nature, the NSP-pyrene tends to aggregate in the aqueous solutions. So the NSP-pyrene was not dispersed well in aqueous solution. Nevertheless, the excited wavelength of 350 nm was chosen for the following experiments.

Interaction between NSP Hybrids and Bacteria. To establish the detection ability for bacteria, the two hybrids of NSP-PHEMA-HA and NSP-pyrene were allowed to be in contact with *E. coli* and *S. aureus*. The change in photoluminescent spectra (PL) was observed when the NSP-PHEMAs were treated with *E. coli*. In Figure 4a, the fluorescent intensities were lower compared to the original fluorescent signal of NSP-PHEMA-HA. Also, the decreases in the fluorescent intensities become more evident when the concentrations of *E. coli* were increased. It was because the NSP-PHEMA-HAs were attached and then aggregated on the surface of *E. coli*. The fluorescent functional groups were shielded and the fluorescent intensities decreased accordingly. The same outcomes were observed when the NSP-PHEMA-HAs were treated with *S. aureus* (Figure 4b). Moreover, the peaks of PL were red shift which could also verify that the aggregation of the fluorescent functional groups took place after

DOI: 10.1021/acsami.5b00796
ACS Appl. Mater. Interfaces 2015, 7, 10771−10778

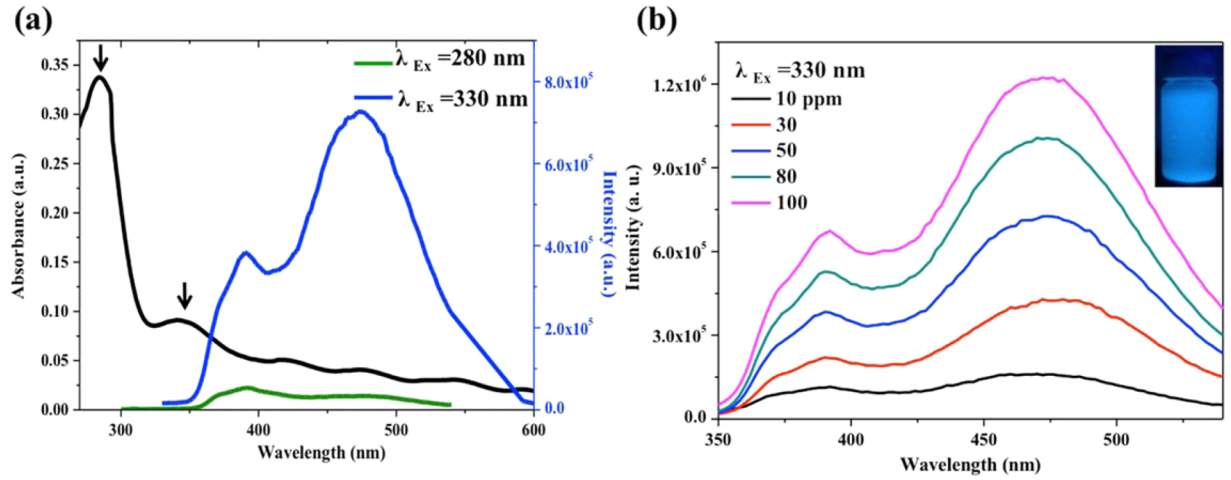

Figure 2. (a) UV−vis spectra (black curve) and photoluminescent spectra (green and blue curves) in different excited wavelength of NSP-PHEMA-HA. (b) The photoluminescent spectra of NSP-PHEMA-HA in different concentration. The inserted part is the photo of compounds under the UV light.

Scheme 2. Conceptual Diagram of Preparation of NSP-Pyrene by Ionic Exchange Reaction

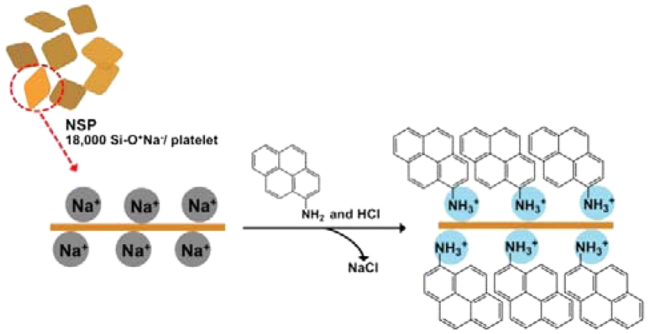

NSP-PHEMA-HAs attaching onto the surface of bacteria.[36] The NSP-pyrenes were also treated with *E. coli* and *S. aureus*. From the PL spectra, the fluorescent intensities only changed slightly when the concentrations of *E. coli* were increased (Figure 4c). Also, no visible changes were observed when NSP-pyrenes were treated with *S. aureus* (Figure 4d). The peaks of fluorescent intensities in PL were irregular. As one can see, these two types of modified NSP, that is, by covalent bonding and ionic exchanging, exhibit different bacteria detection abilities and evidently NSP-PHEMA-HA was more suitable to be applied to biosensors for bacteria detection.

Zeta Potential of NSP and NSP-Pyrene. To understand the reason that the ionic exchanging NSP-pyrene could not detect the bacteria, we used the zeta potential to characterize the ionic properties of NSP and NSP-pyrene (Figure 5). Solutions of 0.01 wt % NSP and NSP-pyrene at different pH were prepared. To adjust the pH, aqueous HCl and NaOH solutions were used. As the pH increased from 3 to 11, the zeta potential of original NSP decreased from −35 to −45. The zeta potential of ionic exchanging NSP-pyrene was similar to NSP when pH was at 5−11. However, it showed an abrupt change from −40 to −15 when the pH decreased from 5 to 3. According to the theory of zeta potential, increased electrostatic repulsion can inhibit agglomeration and settling. A suspension of particles showing a high absolute value of zeta potential is more stable in comparison to suspensions exhibiting low zeta potential.[37,38] As mentioned earlier that ionic exchanging must

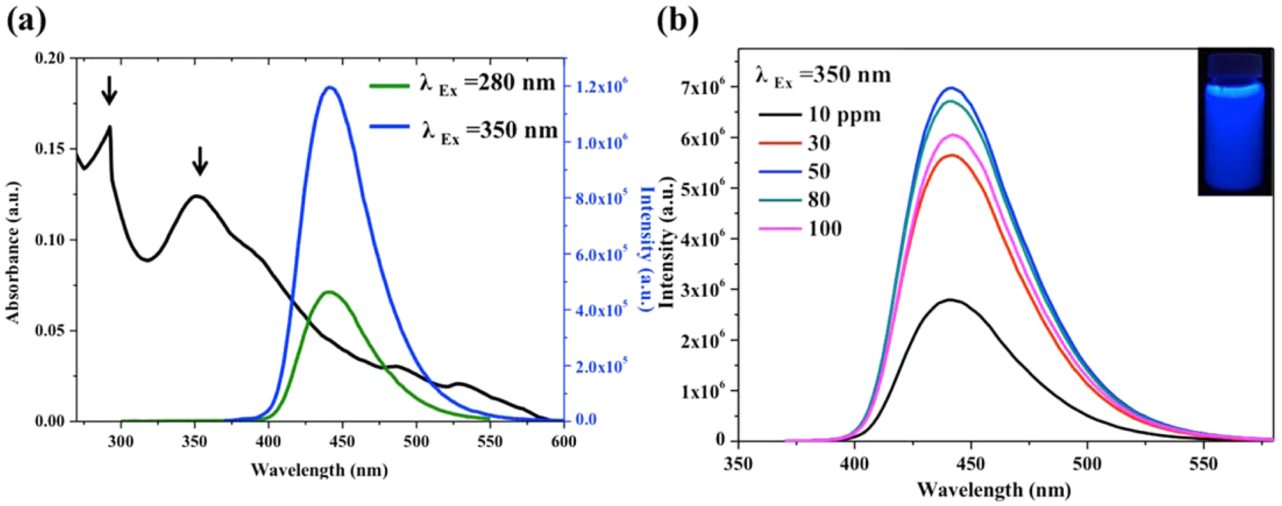

Figure 3. (a) UV−vis spectra (black curve) and photoluminescent spectra (green and blue curves) in different excited wavelength of NSP-pyrene. (b) The photoluminescent spectra of NSP-pyrene in different concentration. The inserted part were the photos of compounds under the UV light.

DOI: 10.1021/acsami.5b00796
ACS Appl. Mater. Interfaces 2015, 7, 10771−10778

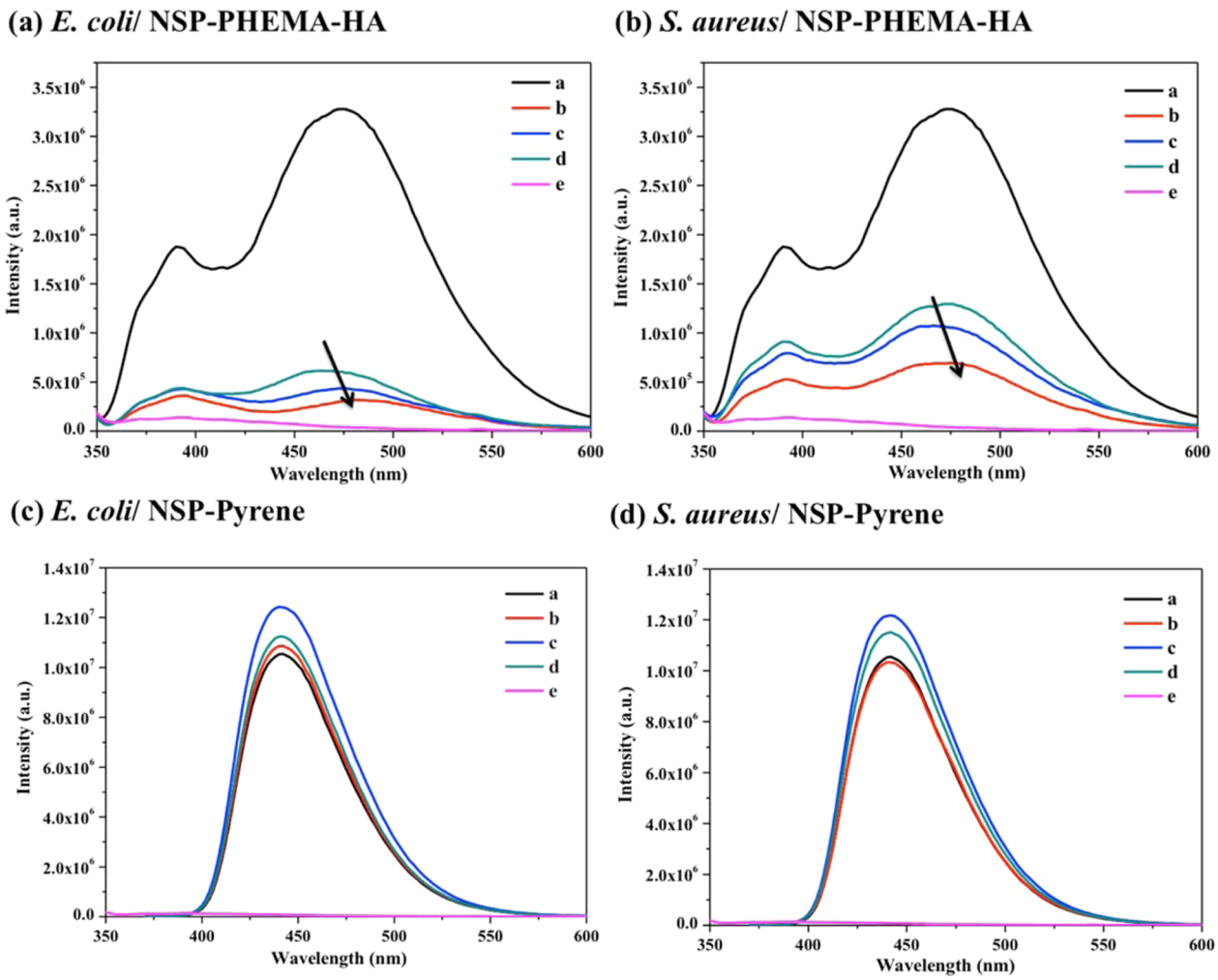

Figure 4. Photoluminescent spectra of NSP-PHEMA-HA and NSP-pyrene with different bacteria, respectively, in which, panel a is NSP-PHEMA-HA (50 ppm) only, panel b is with 10^7 CFU/mL *E. coli* or *S. aureus*, panel c is with 10^6 CFU/mL, panel d is with 10^5 CFU/mL, and panel e is 10^7 CFU/mL *E. coli or S. aureus* only.

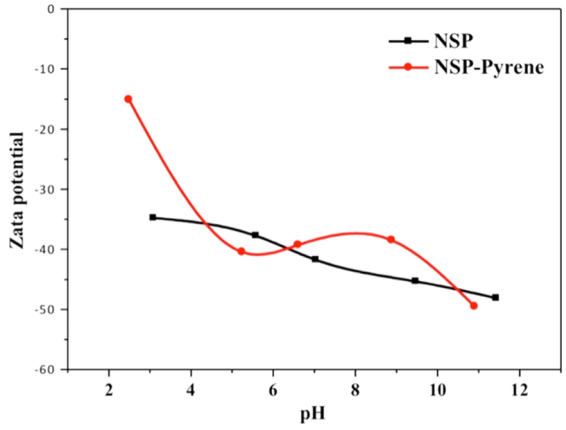

Figure 5. Zeta potential of NSP and NSP-pyrene in different pH.

be performed under acidic environment. When pH was 5−11, it was not acidic enough for the pyrenes to bond to the surfaces of NSPs and therefore the zeta potential of NSP-pyrene was similar to that of NSP. As pH was decreased to 3, the pyrenes became bonded to NSPs and the hydrophobic properties of the pyrenes resulted in significant aggregation of NSP-Pyrenes. The absolute value of zeta potential was then decreased. We speculate that when pH = 7, pyrenes do not bond to NSPs and thus the fluorescence intensities do not change with bacteria concentrations.

Physical Trapping and Detection of NSP-PHEMA-HA. The physical trapping of NSPs is attributed to the large surface area of thin platelets and their intensive ionic surface charges.[16] The ionic charges of NSPs tend to attract polar organic molecules, including organic surfaces of bacteria. However, when we modified the NSP by ionic exchanging to NSP-pyrene, the charges on the surface were shielded. Thus, NSP-pyrene cannot attach itself onto the bacteria. On the other hand, NSP-PHEMA-HAs were obtained by tethering the polymer to the edges of the NSP and covalent bonds would not be influenced by the variation of environmental conditions. The charges on the surface of NSP were kept and can be used to attach to the bacteria. Therefore, the fluorescent intensity decreased when the concentration of bacteria increased (Scheme 3). SEM was performed to directly observe *E. coli* and *S. aureus* before and after treatment with NSP-PHEMA-HAs. As demonstrated clearly in Figure 6, the sheets of NSP-PHEMA-HA were attached to the surfaces of *E. coli* and *S. aureus* as we expected. This outcome distinctly displays that the "physical trapping" of NSP is the specific feature which can be employed to microorganism detection. In the future, NSP can

DOI: 10.1021/acsami.5b00796
ACS Appl. Mater. Interfaces 2015, 7, 10771−10778

Scheme 3. Conceptual Diagram of the Mechanism of NSP-PHEMA-HA and NSP-Pyrene Reacted with Bacteria at pH = 7

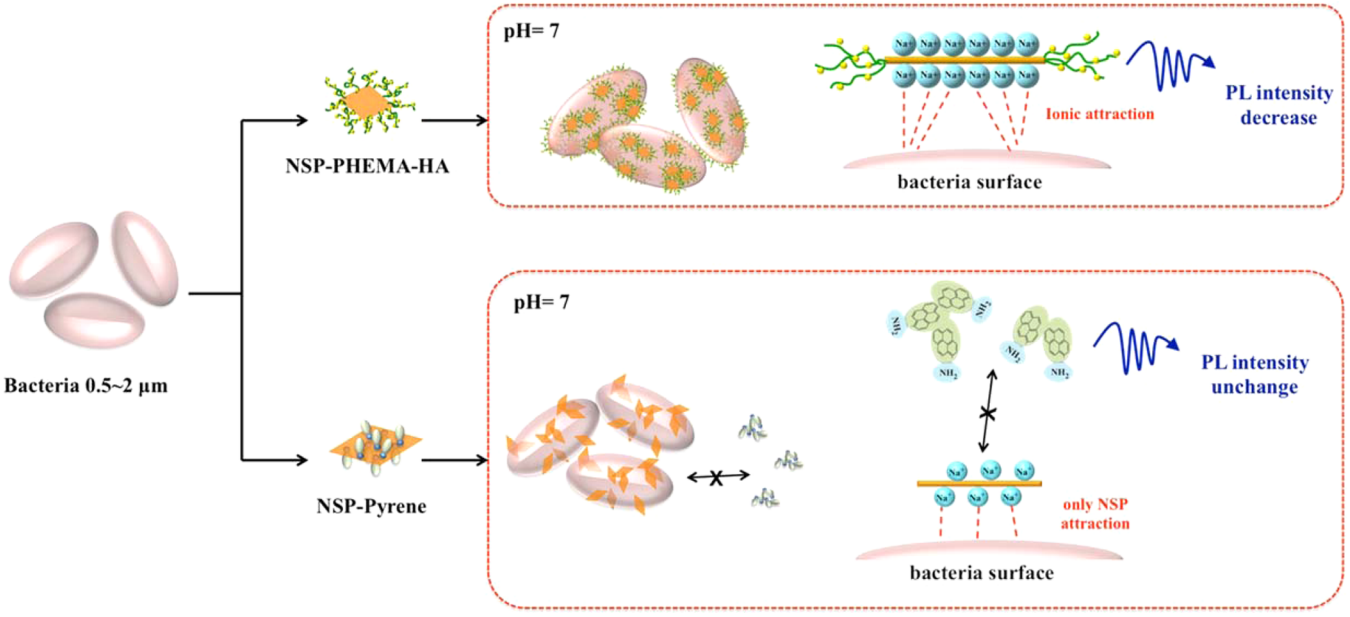

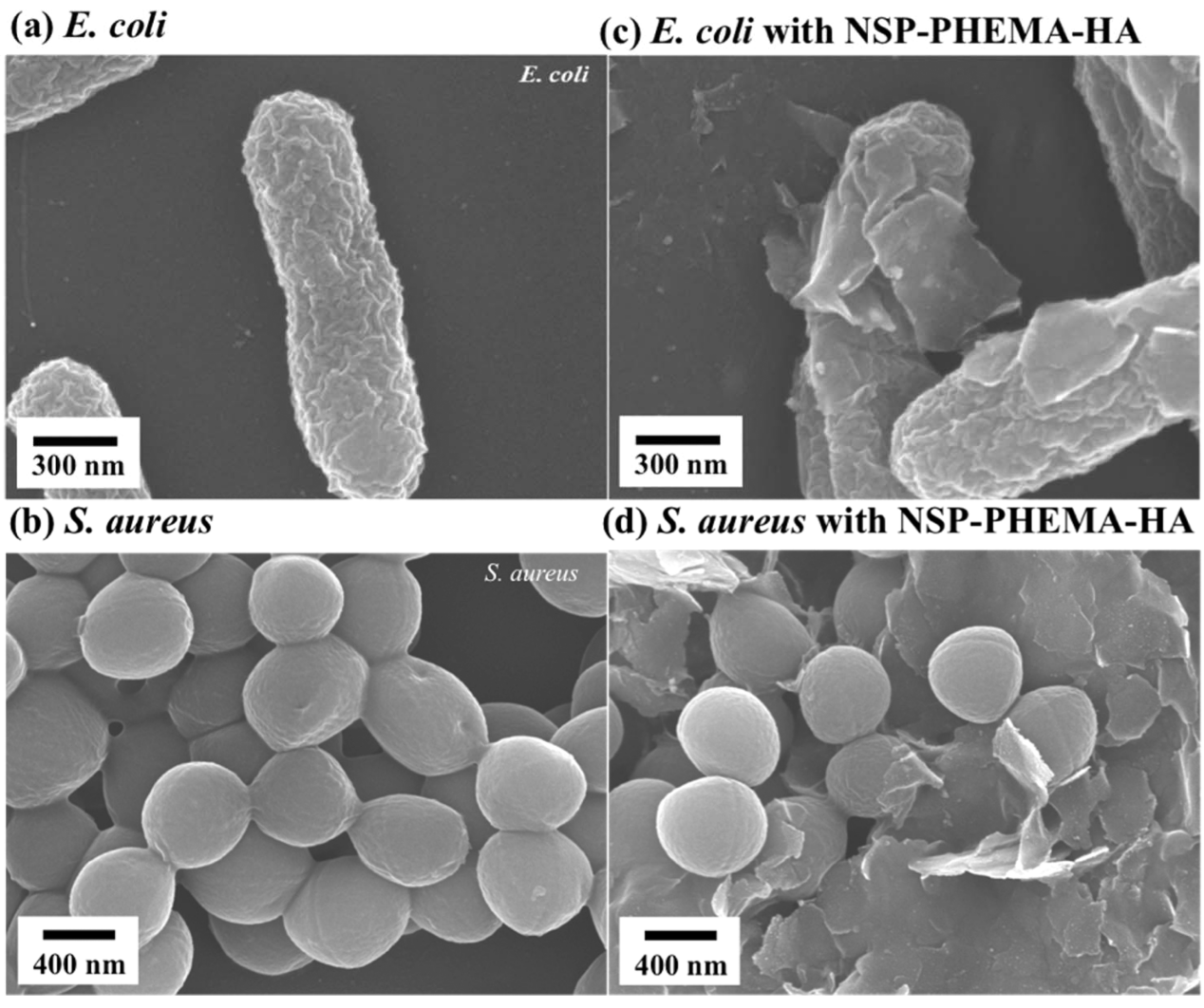

Figure 6. SEM micrographs of original (a) *E. coli* and (b) *S. aureus* and after treatment with NSP-PHEMA-HA (0.005 wt %) over a 1 h ((c) *E. coli* and (d) *S. aureus*).

DOI: 10.1021/acsami.5b00796
ACS Appl. Mater. Interfaces 2015, 7, 10771−10778

also be modified with special functional groups that can interact with certain microorganism.

CONCLUSION

A new class of fluorescence-containing silicate nanoplatelets was synthesized by covalently tethering PHEMA polymer onto NSP and followed by associating with nathphalimide-type fluorescence. The covalent bonding approach was proven to be more effective for bacteria detection when compared with the ionic bonding pyrene as the fluorescence on the surface of NSP. The covalent bonding on the edge of NSP allowed the surface charge exposure toward the incoming bacteria. Furthermore, the ability of bacterial capturing of NSP-PHEMA-HA nanohybrids is pH-independent. The detection of bacteria was verified by the change in PL spectral absorption during the process of NSP-PHEMA-HA adhesion onto the bacteria surface and this phenomenon was further corroborated by the direct observation from SEM.

ASSOCIATED CONTENT

Supporting Information

Materials and procedure for preparing NSP-PHEMA hybrids. The Supporting Information is available free of charge on the ACS Publications website at DOI: 10.1021/acsami.5b00796.

AUTHOR INFORMATION

Corresponding Authors

*Tel: +886-2-3366-5312. Fax: +886-2-3366-5237. E-mail address: jianglin@ntu.edu.tw.

*Tel: +886-2-3366-3014. E-mail: yjsheng@ntu.edu.tw.

Notes

The authors declare no competing financial interest.

ACKNOWLEDGMENTS

We acknowledge financial supports from the Ministry of Science and Technology and the Ministry of Economic Affairs of Taiwan.

REFERENCES

(1) Ivnitski, D.; Abdel-Hamid, I.; Atanasov, P.; Wilkins, E. Biosensors for Detection of Pathogenic Bacteria. *Biosens. Bioelectron.* **1999**, *14*, 599−624.

(2) Disney, M. D.; Zheng, J.; Swager, T. M.; Seeberger, P. H. Detection of Bacteria with Carbohydrate-Functionalized Fluorescent Polymers. *J. Am. Chem. Soc.* **2004**, *126*, 13343−13346.

(3) Willis, R. C. A Review on Some Methods for Pathogen Detection. *Mod. Drug Discovery* **2004**, 36.

(4) Yu, L. S. L.; Reed, S. A.; Golden, M. J. G. Time-Resolved Fluorescence Immunoassay (TRFIA) for the Detection of *Escherichia coli* O157:H7 in Apple Cider. *J. Microbiol. Methods* **2002**, *49*, 63−68.

(5) Nakamura, N.; Burgess, J. G.; Yagiuda, K.; Kudo, S.; Sakaguchi, T.; Matsunaga, T. Detection and Removal of Eg Using Fluorescein Isothiocyanate Conjugated Monoclonal Antibody Immobilized on Bacterial Magnetic Particles. *Anal. Chem.* **1993**, *65*, 2036−2039.

(6) Yamaguchi, N.; Sasada, M.; Yamanaka, M.; Nasu, M. A Simple Way of Quantifying Immunostained Cell Nuclei on the Whole Histologic Section. *Cytometry* **2003**, *54A*, 27−35.

(7) Jung, W. S.; Kim, S.; Hong, S. I.; Min, N. K.; Lee, C. W.; Peak, S. H. DNA Probe Chip System for Multiple Detection of Food Poisoning Microorganisms. *Mater. Sci. Eng., C* **2004**, *24*, 47−51.

(8) Stender, H.; Oliveria, K.; Rigby, S.; Bargoot, F.; Coull, J. Rapid Detection, Identification, and Enumeration of *Escherichia coli* by Fluorescence In Situ Hybridization Using an Array Scanner. *J. Microbiol. Methods* **2001**, *45*, 31−39.

(9) Goodridge, L.; Chen, J.; Griffiths, M. The Use of a Fluorescent Bacteriophage Assay for Detection of *Escherichia coli* O157:H7 in Inoculated Ground Beef and Raw Milk. *Int. J. Food Microbiol.* **1999**, *47*, 43−50.

(10) Robert, F. Nanotechnology: Can High-Speed Tests Sort Out Which Nanomaterials Are Safe? *Science* **2008**, *321*, 1036−1037.

(11) Goodman, T. T.; Ng, C. P.; Pun, S. H. 3-D Tissue Culture Systems for the Evaluation and Optimization of Nanoparticle-Based Drug Carriers. *Bioconjugate Chem.* **2008**, *19*, 1951−1959.

(12) De Cristofaro, A.; Violante, A. Effect of Hydroxy-Aluminium Species on the Sorption and Interlayering of Albumin onto Montmorillonite. *Appl. Clay Sci.* **2001**, *19*, 59−67.

(13) Shan, D.; Yao, W.; Xue, H. Amperometric Detection of Glucose with Glucose Oxidase Immobilized in Layered Double Hydroxides. *Electroanalysis* **2006**, *18*, 1485−1491.

(14) Lin, J. J.; Wei, J. C.; Tsai, W. T. Layered Confinement of Protein in Synthetic Fluorinated Mica via Stepwise Polyamine Exchange. *J. Phys. Chem. B* **2007**, *111*, 10275−10280.

(15) Lin, J. J.; Wei, J. C.; Juang, T. Y.; Tsai, W. T. Preparation of Protein−Silicate Hybrids from Polyamine Intercalation of Layered Montmorillonite. *Langmuir* **2007**, *23*, 1995−1999.

(16) Wei, J. C.; Yen, Y. T.; Su, H. L.; Lin, J. J. Inhibition of Bacterial Growth by the Exfoliated Clays and Observation of Physical Capturing Mechanism. *J. Phys. Chem. C* **2011**, *115*, 18770−18775.

(17) Olphen, H. V. *Clay Colloid Chemistry*, 2nd ed; John Wiley & Sons: New York, 1997.

(18) Theng, B. K. G. *The Chemistry of Clay−Organic Reaction*, 2nd ed; John Wiley & Sons: New York, 1974.

(19) Lin, S.; Lee, C. K.; Lee, S. Y.; Kao, C. L.; Lin, C. W.; Wang, A. B.; Hsu, S. M.; Huang, L. S. Surface Ultrastructure of SARS Coronavirus Revealed by Atomic Force Microscopy. *Cell. Microbiol.* **2005**, *7*, 1763−1770.

(20) Ozdemir, G.; Limoncu, M. H.; Yapar, S. The Antibacterial Effect of Heavy Metal and Cetylpridinium-Exchanged Montmorillonites. *Appl. Clay Sci.* **2010**, *48*, 319−323.

(21) Chu, C. C.; Chiang, M. L.; Tsai, C. M.; Lin, J. J. Exfoliation of Montmorillonite Clay by Mannich Polyamines with Multiple Quaternary Salts. *Macromolecules* **2005**, *38*, 6240−6243.

(22) Lin, J. J.; Chu, C. C.; Chiang, M. L.; Tsai, W. C. First Isolation of Individual Silicate Platelets from Clay Exfoliation and Their Unique Self-Assembly into Fibrous Arrays. *J. Phys. Chem. B* **2006**, *110*, 18115−18120.

(23) Lin, J. J.; Chu, C. C.; Chou, C. C. Self-Assembled Nanofibers from Random Silicate Platelets. *Adv. Mater.* **2005**, *17*, 301−304.

(24) Fan, X.; Xia, C.; Advincula, R. C. Grafting of Polymers from Clay Nanoparticles via In Situ Free Radical Surface-Initiated Polymerization: Monocationic versus Bicationic Initiators. *Langmuir* **2003**, *19*, 4381−4389.

(25) Zhou, Q.; Fan, X.; Xia, C.; Mays, J.; Advancular, R. Living Anionic Surface Initiated Polymerization (SIP) of Styrene from Clay Surfaces. *Chem. Mater.* **2001**, *13*, 2465−2467.

(26) Weimer, M. W.; Chen, H.; Giannelis, E. P.; Sogah, D. Y. Direct Synthesis of Dispersed Nanocomposites by In Situ Living Free Radical Polymerization Using a Silicate-Anchored Initiator. *J. Am. Chem. Soc.* **1999**, *121*, 1615−1616.

(27) Di, J.; Sogah, D. Y. Exfoliated Block Copolymer/Silicate Nanocomposites by One-Pot, One-Step In-Situ Living Polymerization from Silicate-Anchored Multifunctional Initiator. *Macromolecules* **2006**, *39*, 5052−5057.

(28) Shah, D.; Fytas, G.; Vlassopoulos, D.; Di, J.; Sogah, D. Y.; Giannelis, E. P. Structure and Dynamics of Polymer-Grafted Clay Suspensions. *Langmuir* **2005**, *21*, 19−25.

(29) Zhao, H.; Shipp, D. A. Preparation of Poly(Styrene-block-butyl acrylate) Block Copolymer−Silicate Nanocomposites. *Chem. Mater.* **2003**, *15*, 2693−2695.

(30) Sedjo, R. A.; Mirous, B. K.; Brittain, W. J. Synthesis of Polystyrene-block-poly(methyl methacrylate) Brushes by Reverse Atom Transfer Radical Polymerization. *Macromolecules* **2000**, *33*, 1492−1493.

DOI: 10.1021/acsami.5b00796
ACS Appl. Mater. Interfaces 2015, 7, 10771−10778

(31) Wheeler, P. A.; Wang, J.; Baker, J.; Mathias, L. J. Synthesis and Characterization of Covalently Functionalized Laponite Clay. *Chem. Mater.* **2005**, *17*, 3012−3018.
(32) Wheeler, P. A.; Wang, J.; Mathias, L. J. Poly(Methyl Methacrylate)/Laponite Nanocomposites: Exploring Covalent and Ionic Clay Modifications. *Chem. Mater.* **2006**, *18*, 3937−3945.
(33) Chen, Y. M.; Lin, H. C.; Hsu, R. S.; Hsieh, B. Z.; Su, Y. A.; Sheng, Y. J.; Lin, J. J. Thermoresponsive Dual-Phase Transition and 3D Self-Assembly of Poly(N-Isopropylacrylamide) Tethered to Silicate Platelets. *Chem. Mater.* **2009**, *21*, 4071−4079.
(34) Li, P. R.; Wei, J. C.; Chiu, Y. F.; Su, H. L.; Peng, F. C.; Lin, J. J. Evaluation on Cytotoxicity and Genotoxicity of the Exfoliated Silicate Nanoclay. *ACS Appl. Mater. Interfaces* **2010**, *2*, 1608−1613.
(35) Meakin, J. R.; Hukins, D. W. L; Aspden, R. M.; Imrie, C. T. Rheological Properties of Poly(2-Hydroxyethyl Methacrylate) (pHEMA) as a Function of Water Content and Deformation Frequency. *J. Mater. Sci.: Mater. Med.* **2003**, *14*, 783−787.
(36) Nguyen, T. Q.; Doan, V.; Schwartz, B. J. Conjugated Polymer Aggregates in Solution: Control of Interchain Interactions. *J. Chem. Phys.* **1999**, *110*, 4068−4078.
(37) Hanaor, D.; Michelazzi, M.; Leonelli, C.; Sorrell, C. C. The Effects of Carboxylic Acids on the Aqueous Dispersion and Electrophoretic Deposition of ZrO_2. *J. Eur. Ceram. Soc.* **2012**, *32*, 235−244.
(38) Jan, K. M.; Chien, S. Influence of the Ionic Composition of Fluid Medium on Red Cell Aggregation. *J. Gen. Physiol.* **1973**, *61*, 665−668.

DOI: 10.1021/acsami.5b00796
ACS Appl. Mater. Interfaces 2015, 7, 10771−10778